MAGMATIC FOAM: COMPUTATIONAL MULTIPHYSICS MODELING OF MULTIPHASE FLOWS AND PLANETARY AMBIENT EFFECTS. S E. H. Sakimoto[1,2], T. K. P. Gregg[2], and D. H. Needham[3], [1]Space Science Institute, 4765 Walnut Street, Suite B, Boulder, CO, 80301 (susansakimoto@gmail.com), [2]126 Cooke Hall, Department of Geology, University at Buffalo, Buffalo, NY 14260 (tgregg@buffalo.edu.), [3]NASA's Marshall Space Flight Center, ST13/NSSTC 2064, 320 Sparkman Dr. Huntsville, AL 35805 (debra.m.hurwitz@nasa.gov).

Introduction: Magmatic foam is suggested to play a significant role in multiple planetary volcanic processes, and its presence or absence is interpreted to be key in interpreting resulting landscape feature morphology, crater retention, and longevity. Prior modeling efforts have commonly relied upon a series of linear approximations for ease and simplicity, which introduces cumulative errors and uncertainty. We model several detailed aspects of magmatic foam formation and transport that are expected to be pivotal or rate-limiting in determining when and where magmatic foams are present in volcanic processes.

Background: Most volcanic eruption products throughout the Solar System were not observed during emplacement, so eruption and emplacement characteristics need to be inferred from the static resulting morphology. Recent investigations into lunar lava mounds, particularly within the irregular mare patch previously named Ina-D [1-6] have reinvigorated the study of how lava's behavior changes when it contains enough vesicles to be considered mechanically as a "foam" (≥95 vol.% bubbles) instead of as a liquid [7-9]. These hypotheses recall the suggestion that Venus' circular, flat-lying, steep-sided "pancake domes" were also the product of excessively vesicular basaltic lavas [e.g., 10]. On Earth, the eruption of vesicle-rich rhyolite lava on the sea floor from the Havre volcano in the southwest Pacific in 2012 [e.g., 11] clearly demonstrated that not only does vesicle-rich rhyolite lava behave very differently from basaltic lavas, but that ambient conditions are key in eruption and emplacement behaviors.

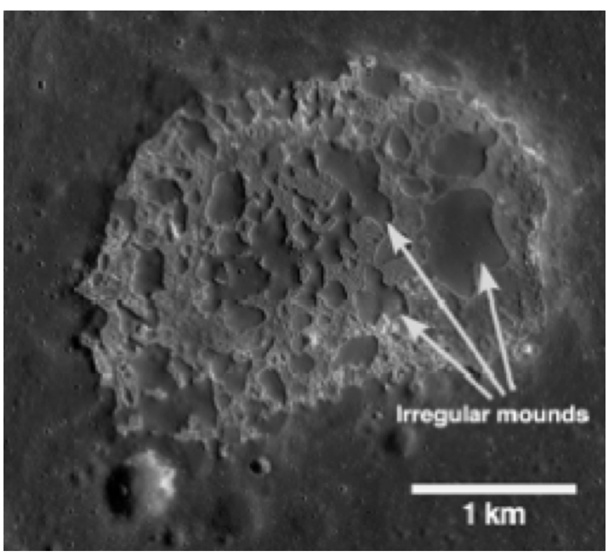

Figure 1. LROC NAC image M11985703LC of the Ina depression (resolution of 0.5 m/pixel) showing smooth dark irregular mounds approximately 10 m high. PDS3 data set LRO-L-LROC-3-CDR-V1.0.

Figure 1 shows a portion of Lunar Reconnaissance Orbiter Camera (LROC) narrow angle image M119815703 for Ina-D (a.k.a. "irregular mare patch Ina"), a depression at the summit of a lunar volcanic dome at 18°40'N, 5°18'E. Garry et al. [5] suggested that these irregular mounds were the result of a lava flow inflation process, while others [e.g., 7, 12, 13] suggest that they are remnants of extruded magmatic foams within a lava lake. Braden et al. [14] interpret the crater size frequency distributions to reflect a relatively young age of <100 Ma, whereas others [3] suggest ages as young as 10 Ma or as old as ~3.5 Ga [12]. The older estimates assume a magmatic foam material with atypical crater retention properties [7 - 9, 12, 15, 16]. Here, we quantitatively model aspects of the proposed magmatic foam eruption processes to better constrain the likelihoods of magmatic foam eruption as well as foam eruption product material properties.

Methods: We use COMSOL Multiphysics® software with the computational fluid dynamics (CFD) [17], subsurface, and heat-flow modules to calculate temperature and velocity fields and wall shear stresses for Newtonian and non-Newtonian magma rheologies. In particular, we simulate three key processes. First, we model the dike and conduit flow of Bingham plastic materials [8, 18] for both highly silicic and basaltic foam parameter values. Second, we model the two-phase conduit and dike flow of a foam above a rising magma for proposed late-stage eruptions of magmatic foams, a mechanism suggested as responsible for forming Irregular Mare Patches (IMPs) and other possible foam-containing deposits. Third, we model ascent of bubbles, which are proposed to collect in the tips of dikes [8, 18-21] during dike propagation for slow ascent rates [22, 23].

Model Suite A) Computational simulation of Bingham materials in dike and conduit flow. This model compares common Bingham flow approximations for isothermal crack and conduit ascent [e.g. 18] with full computational laminar flow solutions then assesses solution differences between the two approaches.

Model Suite B) Computational simulation of two-phase flow for magma and magmatic foam. Here, we model the slow ascent of two-phase flow (magma + bubbles) with an overlying magma foam and consider the predicted velocity fields, the fluid interface tracked by moving mesh deformation, and wall shear rates.

Model Suite C) Computational simulation of bubble ascent. Experimental and computational studies suggest that bubble nucleation, growth, and disruption all depend on shear rate as well as magma viscosity, density, and vesicle properties [23-25]; also the presence of a local or widespread impermeable "skin" preventing volatile losses [e.g. 2] may be significant. In this model, we consider bubble ascent through several magmatic compositions using a two-phase flow simulation tracking the moving mesh interface between the gas-filled dike tip and the degassing magma as a function of ambient conditions and ascent rate for a constant-width near surface dike with different planetary pressure conditions.

Results and Discussion: Figure 2 shows the computational model geometry and material domains for these three magmatic foam model suites.

Results from model suite A suggest that common linear approximations for Bingham flow in dikes and conduits for flow rates may be as accurate to within 10% of full velocity field solutions or inaccurate by an order of magnitude (or more). Accuracy depends strongly on material parameter ranges, rheology relationships and geometry complexity.

Results from model suite B (two-phase magma and foam flow with a deformable fluid boundary) suggest that foam commonly does not passively rise above the magma in conduit and dike flow, and that boundary and rheology effects add: significant complexity, foam loss and breakdown, and velocity-dependent volume fractions of material ratios. There is a strong dependence on geometry, rheology, and strain rates.

Results from model suite C (bubble ascent) suggest that rheology-dependent magmatic bubble segregation is more sensitive to ambient conditions and shear-rate-dependent factors than previously thought.

Acknowledgments: This study used images from PDS3 data set LRO-L-LROC-3-CDR-V1.0.

References: [1] Whitaker E.A. (172), *NASA SP 289*, 25-84-25-85. [2] Evans R.E. and El-Baez F. (1973) *NASA SP 330*, 30-13-30-17. [3] Schultz P. et al. (2006) *Nature,* 444, 184–186. [4] Staid M. et al. (2011) *LPSC XLII,* Abstract #2499. [5] Garry W.B. et al. (2012) *JGR* 117, E00H31. [6] Stopar J.D. et al. (2019) *Planetary Space Sci.*, 171,1-16. [7] Wilson L. and Head J.W. (2017) *JVGR*, 335, 113-127. [8] Wilson L. and Head. J.W. (2017) *Icarus,* 283, 146-175. [9] Wilson L. et al. (2019) *JVGR,* 374, 160-180. [10] Pavri B. et al. (1992) *JGR* 97(E8),13,445-13,478. [11] Jutzeler M. et al. (2014) Nature Communications 5, #3660. [12] Qiao L. et al. (2017) *Geology*, 45, 455-458. [13] Qiao L. et al. (2019) JGR, 124, 1100-1140. [14] Braden S.E. et al. (2014) *Nat. Geosci.,* 7, 787–791. [15] Head J.W. and Wilson L. (2017) *Icarus,* 283, 176-223. [16] Wilson L. and Head J.W. (2018) *GRL*, 45, 5852-5859. [17] COMSOL Multiphysics® v. 5.5 (2019) www.comsol.com COMSOL AB, Stockholm, Sweden. [18] Wilson L. and Head J.W. (2003) *GRL*, 30, 1605. [19] Head J.W. et al. (2002) *JGR,* 107(E1), 5001. [20] Jozwiak L.M. et al (2017) *Icarus,* 283, 224-231. [21] Namiki A. Et al. (2019) *JVGR*, 106760. [22] Rutherford, M.J and Gardner J.E. (2000) Encyclopedia of Volcanoes, 207-217. [23] Martel C. Et al. (2017) *Volcanic Unrest:Advan.Volc.*, Springer. [24] Schauroth J. et al. (2018) *EGU2018*, 1031. [25] Ryan A.G. et al., (2019) *JGR,* 124, 8167-8186. [26] von Aulock F.W. et al. (2017) Front. Earth Sci., 5, 46.

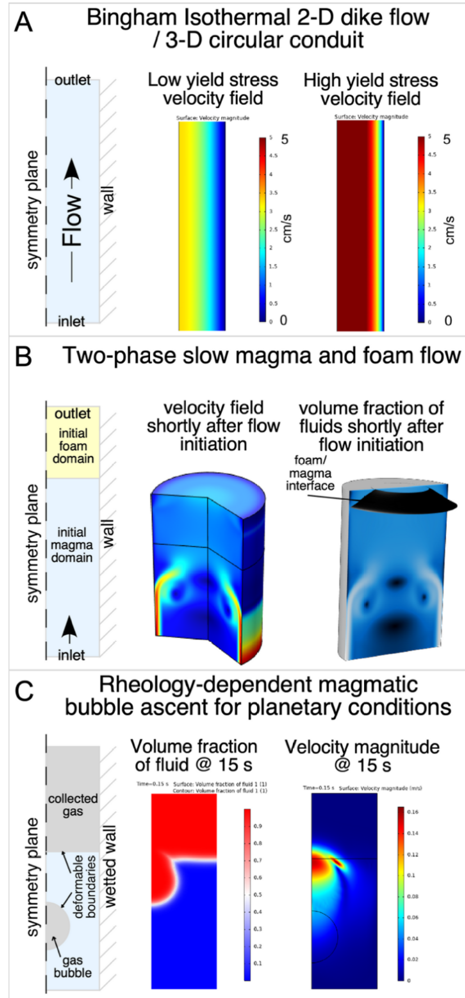

Figure 2. Computational model geometry domains and solution examples for A) Bingham dike and conduit flow, B) Two-phase magma and foam flow, and C) Two-phase flow bubble ascent and gas accumulation.